ENVIRONMENTAL FATE OF TOXIC CHEMICALS ON SURFACE MATERIALS IN LABORATORY WIND TUNNELS: MEASURED AND COMPUTED WIND SPEEDS AND FLOW FIELDS

Daniel Weber and John Molnar
Edgewood Chemical Biological Center

Wendel Shuely
GEO-Centers, Gunpowder POB 68
APG, MD 21010-5424

ABSTRACT

An understanding of the fate and effects of chemical agents on material surfaces under environmental conditions is becoming critical as the probability of contamination increases for military and civilian airports and seaports and Homeland targets. The methodology is not available for measuring the fundamental evaporation, desorption, and decomposition of chemical agents as a function of time in a controlled laboratory wind tunnel. The methodologies under development can be classified by the instrumental approaches as based on microbalances, vapor analysis, photo-imaging of droplet contact angle cross-sections, or combined methods. All approaches have a common requirement for well-characterized flow fields for the droplet in the laboratory wind tunnel geometry. The microbalance methodology described will be based on horizontal balances in a conventional mode, horizontal balance in the reverse flow mode for higher wind speeds, a vertical microbalance in evolved-gas, quasi-horizontal mode, and dual a beam differential thermal instrument mode. Two parallel approaches are being pursued to characterize the aerodynamic behavior in laboratory wind tunnels. Direct measurements are being performed of wind speed as a function of position relative to the agent droplet on the surface. Hot wire anemometry and micro-positioning devices are being employed for the measurements. Special calibration techniques were applied to extend the anemometer measurements to low wind speeds. Computational Fluid Dynamic (CFD) methods are being applied to the microbalance and vapor sampling wind tunnel geometries to complement the measured wind speeds and profile shapes. The overall emphasis is on transfer of robust data sets of agent residual mass and vapor concentration as a function of time at known wind speeds for models supporting battlefield decisions

INTRODUCTION

The research objective is to understand the variables that control the volatilization of toxic chemical contaminants from material surfaces into the environment. This time dependent distribution of vapor and residual surface liquid determines the inhalation and contact hazard, respectively. A mass balance that includes measurements of the fraction irreversibly sorbed or

Report Documentation Page

Form Approved
OMB No. 0704-0188

1. REPORT DATE	2. REPORT TYPE	3. DATES COVERED
01 JUL 2003	**N/A**	**-**

4. TITLE AND SUBTITLE	5a. CONTRACT NUMBER
Environmental Fate Of Toxic Chemicals On Surface Materials In Laboratory Wind Tunnels: Measured And Computed Wind Speeds And Flow Fields	5b. GRANT NUMBER
	5c. PROGRAM ELEMENT NUMBER
6. AUTHOR(S)	5d. PROJECT NUMBER
	5e. TASK NUMBER
	5f. WORK UNIT NUMBER
7. PERFORMING ORGANIZATION NAME(S) AND ADDRESS(ES) **Edgewood Chemical Biological Center APG, MD 21010-5424**	8. PERFORMING ORGANIZATION REPORT NUMBER
9. SPONSORING/MONITORING AGENCY NAME(S) AND ADDRESS(ES)	10. SPONSOR/MONITOR'S ACRONYM(S)
	11. SPONSOR/MONITOR'S REPORT NUMBER(S)

12. DISTRIBUTION/AVAILABILITY STATEMENT
Approved for public release, distribution unlimited

13. SUPPLEMENTARY NOTES
See also ADM001523., The original document contains color images.

14. ABSTRACT

15. SUBJECT TERMS

16. SECURITY CLASSIFICATION OF:			17. LIMITATION OF ABSTRACT	18. NUMBER OF PAGES	19a. NAME OF RESPONSIBLE PERSON
a. REPORT	b. ABSTRACT	c. THIS PAGE			
unclassified	**unclassified**	**unclassified**	**UU**	**21**	

decomposed is also an objective. The approach includes the measurement of droplet evaporation at several experimental levels, from single droplet wind tunnels of minimal size, onto larger laboratory wind tunnels fitted into a fume hood, to chamber and large scale wind tunnel tests, and finally to field tests. The goal is to structure the experimental geometry and variable set such that wind tunnel results at each level can be correlated to the degree feasible. Therefore, one needs an initial understanding of the variables that control the volatilization results for each experimental level or scale. The ultimate goal is for each wind tunnel scale to produce time vs. concentration data sets that provide the basis for modeling the hazards from the chemical contaminant. The focus of this evaluation is to measure and calculate the wind speed at the droplet-material interface at ground level for fundamental, small scale, single droplet evaporation/desorption investigations performed in our laboratory (1-3). Several different geometries for laboratory wind tunnels are being designed to provided various ranges of wind speed, vapor concentration, temperature, and humidity and to provide these values within a measurable range for chemical contaminants with a wide range of volatilities, from GD to VX. The geometries studied herein include:

- Horizontal microbalance with tube flow, (TA Instruments Model 951)
- Horizontal microbalance with reversed tube flow (custom TA Instruments Model 951)
- Vertical microbalance with Evolved Gas horizontal flow, (TA Instruments Model 2950)
- Rectangular geometry with droplet at the floor and down-stream vapor analysis (custom)

The microbalance geometries have a sample pan containing the droplet on the surface material suspended in the flow. The rectangular geometry has the droplet on the surface at the floor wall. Therefore, in all cases, the wind velocity is lower than the mean velocity due to the sublayer wall effects, discussed herein.

REVIEW AND ANALYSIS

WIND SPEED AT GROUND LEVEL: THE WIND TUNNEL WALL EFFECTS

In general, wind speed decreases as the distance to the ground or wind tunnel wall decreases (4). The shape of the velocity vs distance profile depends on turbulence and other variables. Most meteorological data on wind speed is apparently measured at various standardized heights, for example 2 meters. The shape of the wind speed vs height (distance to the ground) might be complex and quite variable. The wind speed data available to modelers and battlefield managers utilizing models might be at a variety of heights above ground level. An appropriate experimental strategy would be to measure the wind speed at or near the drop in the droplet wind tunnel and allow current and future modelers to estimate the wind speed at the ground based on wind speed transducers at airports or other sources at greater heights. In the lab, the wind speed would be measured as a function of height above the drop or sorbed agent in the environmental fate wind tunnels. Since some transducers might interfere with the flow field near the drop, one might need to extrapolate from various distances above the drop to the ground or wall level.

The experimental matrix is influenced by the lower wind speed at the wall or ground in that one would employ a lower wind speed range since these would correspond to higher nominal wind speeds at conventional measurement heights. Aerodynamic and wind tunnel expertise is needed to select the range of lower wind speeds at the wall or ground that corresponds to the nominal wind speeds at ca 2 meters. The exact relationship between height and wind speed does not have to be known or assumed, at this time, since the environmental fate measurements are

being performed at several wind speeds and evaporation and desorption rates can be interpolated or modeled as a function of wind speed; it is only necessary to select an appropriate range.

The vapor-sampling wind tunnel contains the drop a ground level. The microbalance drop wind tunnel contains the substrate and drop suspended in the middle of the wind tunnel. The microbalance wind tunnel will cover the lower to mid level wind speeds in the experimental matrix and the ground level vapor sampling wind tunnel will cover the mid to higher wind speeds. An attempt will be made to measure the wind speed at the microbalance drop-surface in addition to the mean wind-speed in the tube. These lower wind speeds are assumed to create droplet evaporation and desorption in the laminar sublayer. Experiments with both configurations at identical wind speeds at the droplet height and other conditions will allow comparisons of these geometry effects.

LOW LEVEL WIND SPEED TRANSDUCERS

The optimum strategy is to measure the velocity near the ground level sessile drop or sorbed drop; however, the current capabilities of wind speed transducers at low level might present a challenge. Even the hot wire anemometer range may not extend to the low levels required for some of the experimental matrix; the lowest wind speed that can be measured is estimated to be about 0.05 m/s, with special calibration methods.

HEIGHT VERSUS WIND VELOCITY RELATIONSHIPS IN ENVIRONMENTAL WIND TUNNELS (5-9)

It has been found that at power law representation of velocity to height provides a good approximation for turbulent atmospheric Boundary layers.

$$\frac{u}{U_{ref}} := \left(\frac{z}{z_{ref}}\right)^{p}$$

u is the mean velocity at height z, and U_{ref} is the reference velocity at height z_{ref}. p is based on roughness; typical values vary between 0.1 and 0.5, with greater roughness yielding higher values of p

Let: $Z_{ratio} := \frac{z}{z_{ref}}$ and $U_{ratio} := \frac{u}{U_{ref}}$ and solve eq. for Z_{ratio}

$$Z_{ratio} := \left(U_{ratio}\right)^{\frac{1}{p}}$$

If various values of p are used, 0.1 (Z_{ratio1}), 0.3 (Z_{ratio2}) and 0.5 (Z_{ratio3}) , the following representative profiles can be produced.

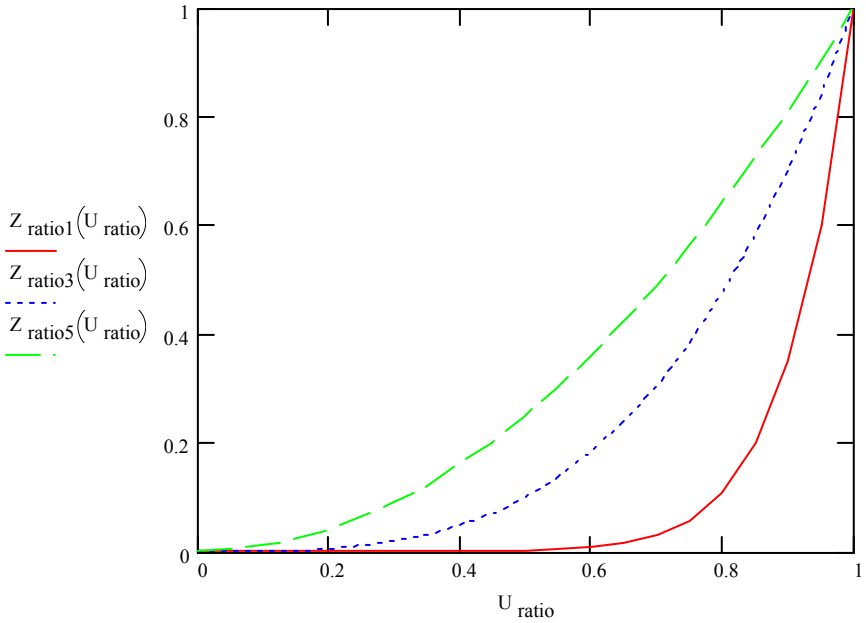

Figure 1. Representative profiles using various p values.

As can be seen in Figure 1 above, an increase in roughness (higher value of p) is associated with an increase in turbulence, which yields greater mixing, and thus a more gradual profile. The value of 1.0 on the y-axis represents the midpoint of the wind tunnel.

Based on some rough assumptions, and using the boundary layer profile power law, an estimate of the corresponding height above the surface that corresponds to a velocity of 0.3 Kph can be made. This velocity is considered an estimate of a typical velocity that can be used in the microbalances. Thus, for a typical 500 m high atmospheric boundary layer with a free stream velocity of 20m/s at 500m, and a value of p = 0.3, the height in the boundary layer corresponding to a velocity of 0.05 Kph is only 0.006 mm. This is extremely close to the surface, and very well could be within the laminar sublayer, however, it must be noted that this calculation is based on the stated input estimates.

EXPERIMENTATION AND RESULTS

We have shown that microbalance instrumentation in wind tunnel geometry can be employed to measure toxic droplet evaporation and desorption from material surfaces. Details of microbalance procedures are provided in previous publications (1-3). In the examples reported here, temperature, average wind speed, and relative humidity were controlled or measured. Microbalance instruments employed were TA Instrument Models 951 and 2950. In general, 5 mg droplets were placed on coated substrates suspended on the sample pan of a thermal microbalance.

A diagram of a droplet on an adsorbing or absorbing polymeric coating is shown in Figure 2. The chemical contaminant droplet falls on a material surface as a droplet. The initial contact angle is shown to decrease as the drop spreads to a near equilibrium contact angle. Evaporation then occurs from: 1) a constant contact angle, or 2) a constant-base with decreasing contact angle, or 3) a mixed mode. Concurrent sorption and wicking is shown and evaporation

from lateral surfaces is indicated. In the final stage, contaminant loss would be at a diffusion-controlled rate by desorption from the material surface.

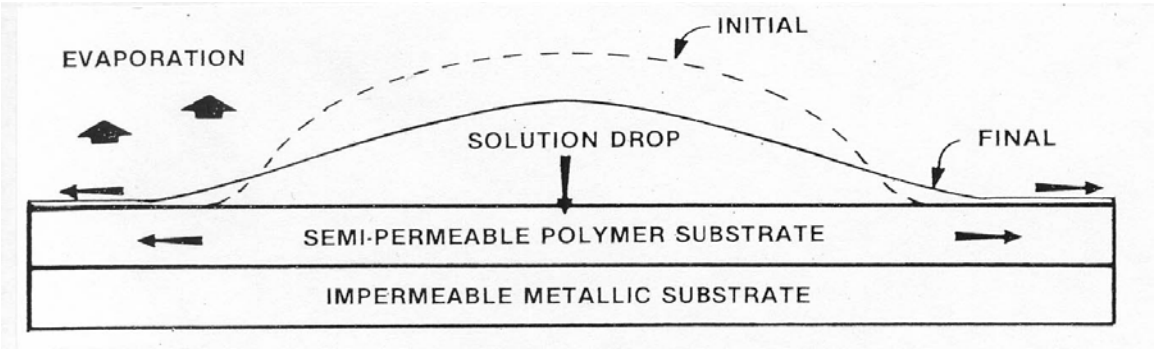

Figure 2. Diagram of a droplet on a polymeric substrate showing the initial and final contact angle and including lateral surface wicking and lateral transport within the substrate; evaporation from the droplet and lateral film is shown.

WIND SPEED MEASUREMENTS AND COMPUTATIONS

A photo of the apparatus for measurement of wind speed profiles as a function of distance from the wind tunnel wall is shown in Figures 3 and 4.

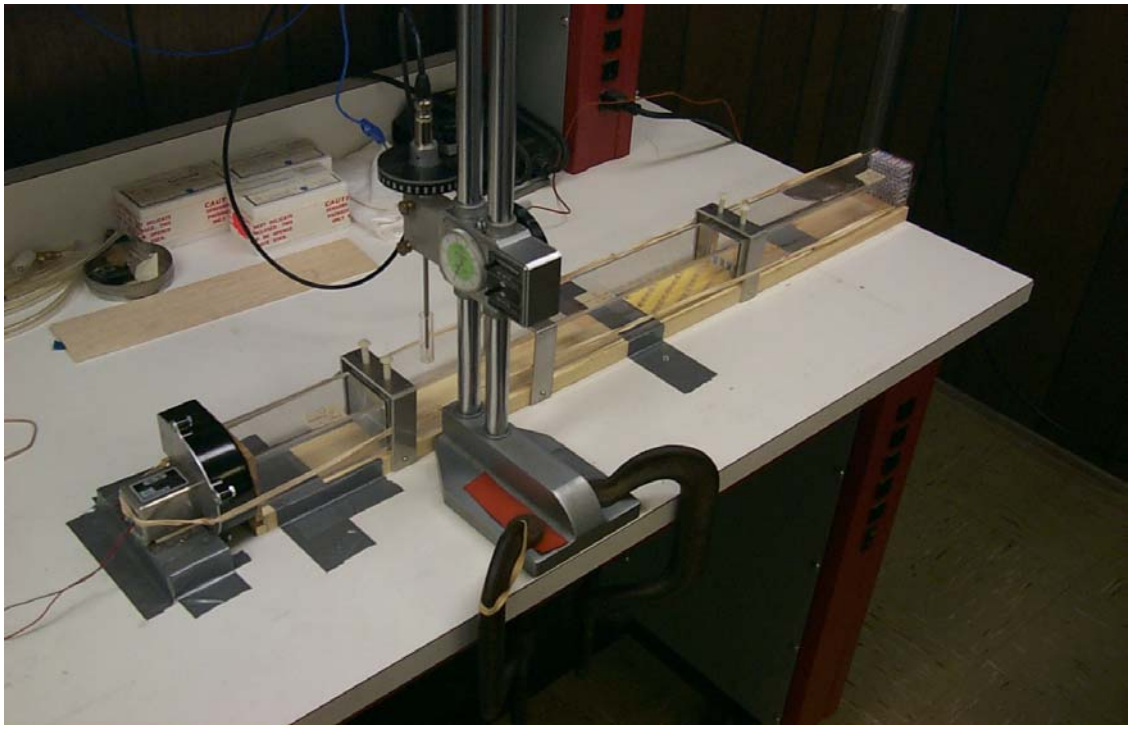

Figure 3. Photograph of a Hot Wire Anemometer Mounted to a Micro-positioning Device: Measurements of Wind Speed Profiles in a Droplet Wind Tunnel Prototype.

The prototype wind tunnel with strakes as turbulence trips and rectangular roughness elements is shown in Figure 4. The micro-positioning device was attached to a small hot wire anemometer that was interfaced to a data acquisition system. Model IFA300, TSI, Minn., MN.) The Computational Fluid Dynamics (CFD) software package is titled CFX and is licensed from AEA Technology Engineering Software, Pittsburgh, PA.

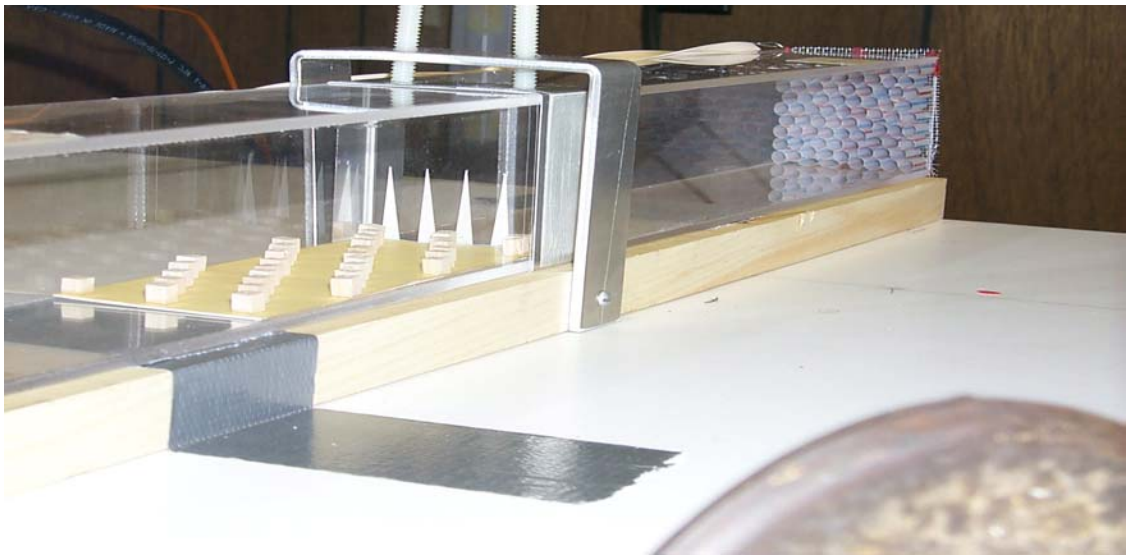

Figure 4. Turbulence Tripping and Roughening Section of Prototype Wind Tunnel for Agent Droplets: Roughness elements (small blocks) are shown in the foreground and turbulent strakes (spikes) to trip the flow are shown in the background. These sections are between the flow contraction section and the sample section.

CAPABILITIES OF MICROBALANCE INSTRUMENTATION

Figures 5 and 6 demonstrate the capability of the microbalance in wind tunnel geometry to measure the evaporation from a droplet with good reproducibility. Figure 7 provides an example comparing the evaporation curve for GD with candidate simulants with similar vapor pressure. Note that the instrument is capable of discriminating amongst the liquids and ranking them in terms of deviation from GD

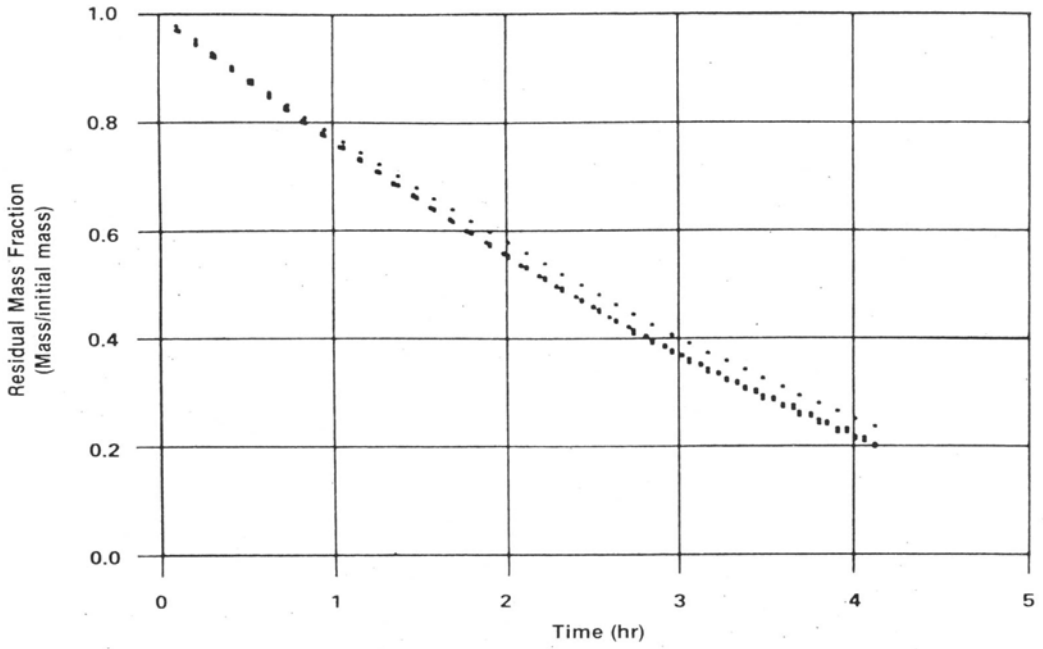

Figure 5. Reproducibility Represented by the Overlay of Five Repetitions for Mass-loss Versus Time Experiments Employing a Horizontal Microbalance in a Wind Tunnel Geometry: *ca* 5 mg Sessile Droplet of Thickened 4-Chloro-n-Butylacetate on a Polyurethane Coating at 24-26 deg C and 0% RH

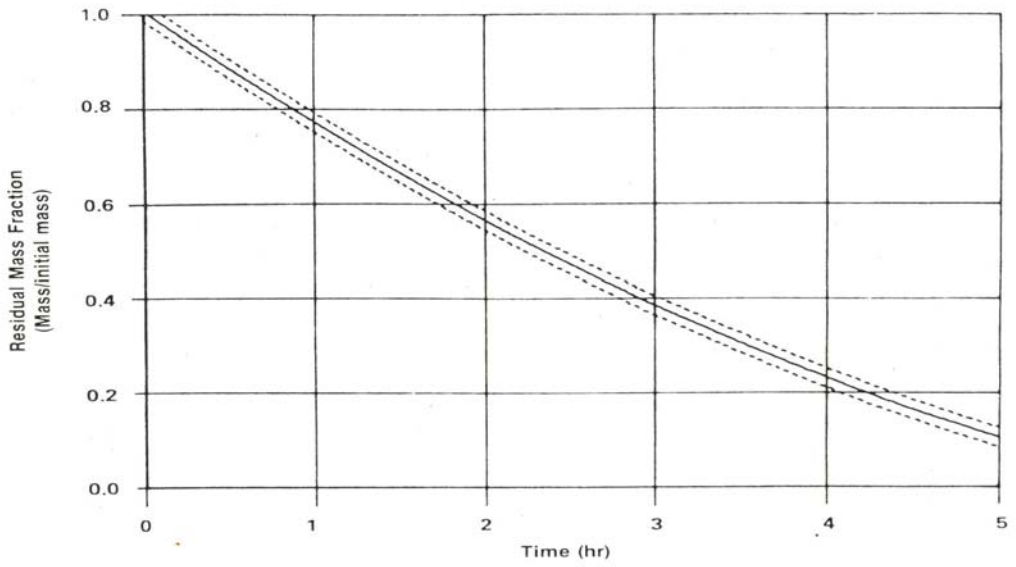

Figure 6. Reproducibility Represented by the 95% Confidence Interval for Mass-loss Versus Time Experiments Employing a Horizontal Microbalance in a Wind Tunnel Geometry: *ca* 5 mg Sessile Droplet of Thickened 4-Chloro-n-Butylacetate on a Polyurethane Coating at 24-26 deg C and 0% RH

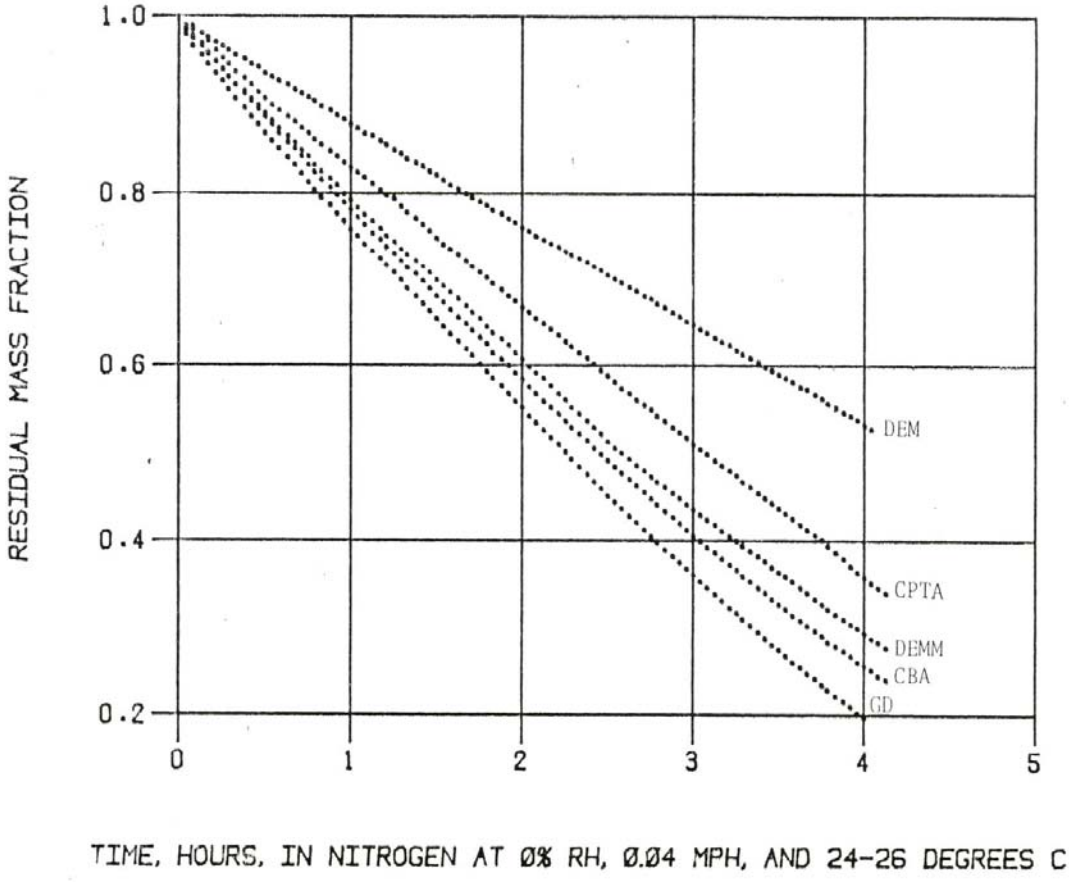

Figure 7. Capability for Discrimination in Evaporation Rate Between GD and Several Neat Liquids with Similar Vapor Pressures Employing a Horizontal Microbalance in a 0.07 KPH Wind Tunnel Geometry: *ca* 5 mg Sessile Droplets on a Polyurethane Coating at 24-26 deg. C and 0% RH:

GD: Pinacolyl methylphosphonofluoridate
CBA: Chlorobutylacetate
DEMM: Diethylethylmalonate
CPTA: Chloropropylthiolacetate
DEM: Diethylmalonate

TUBE FLOW WITH SAMPLE PAN: WIND SPEED MEASUREMENTS AND COMPUTATIONS

The simplest geometry studied was the tube flow with a sample pan centered in the air stream, corresponding to the TA Model 951 microbalance. A photo of the hot wire anemometer measurements is shown in Figure 8. A close-up shows the micro-positioning device with attached hot wire anemometer measuring the flow near the sample pan surface where the contaminant droplet would be deposited. A comparison of the measured versus computed wind velocity profiles is provided in Figure 9.

Figure 8. Experimental Setup For Velocity Measurements Through a Prototype TGA 951 Wind Tunel

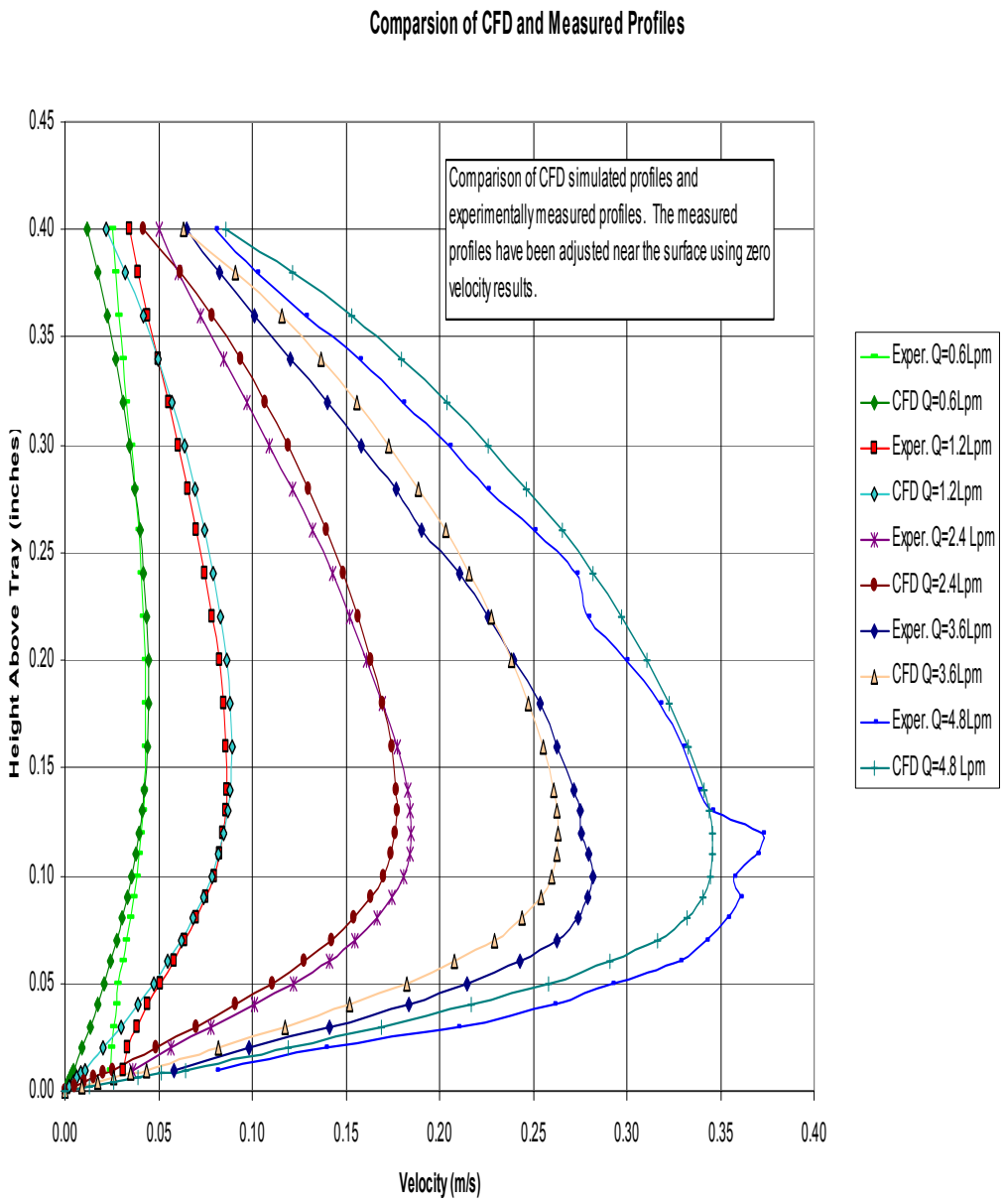

Figure 9. Comparison of Measured Velocity Profiles With Simulated Computational Fluid Dynamics (CFD) Profiles for Flow Rates of 0.6, 1.2, 2.4, 3.6 and 4.8 LPM.

- The comparison is very good between experimental and computational (solid line) results.
- There is some discrepancy near the sample pan surface for the lower flow rates, but this is expected due to the difficulty in making hotwire measurements in this low flow regime

Since these computed profiles almost overlay the measured profiles, the profiles for other coordinates along the droplet sample surface could be calculated with confidence, and these profiles are plotted in Figure 10. Color-coded velocity profiles from the CFD simulation are demonstrated in Figure 11. Note that the droplet surface area has a similar velocity to that at the wall (based on the color calibration).

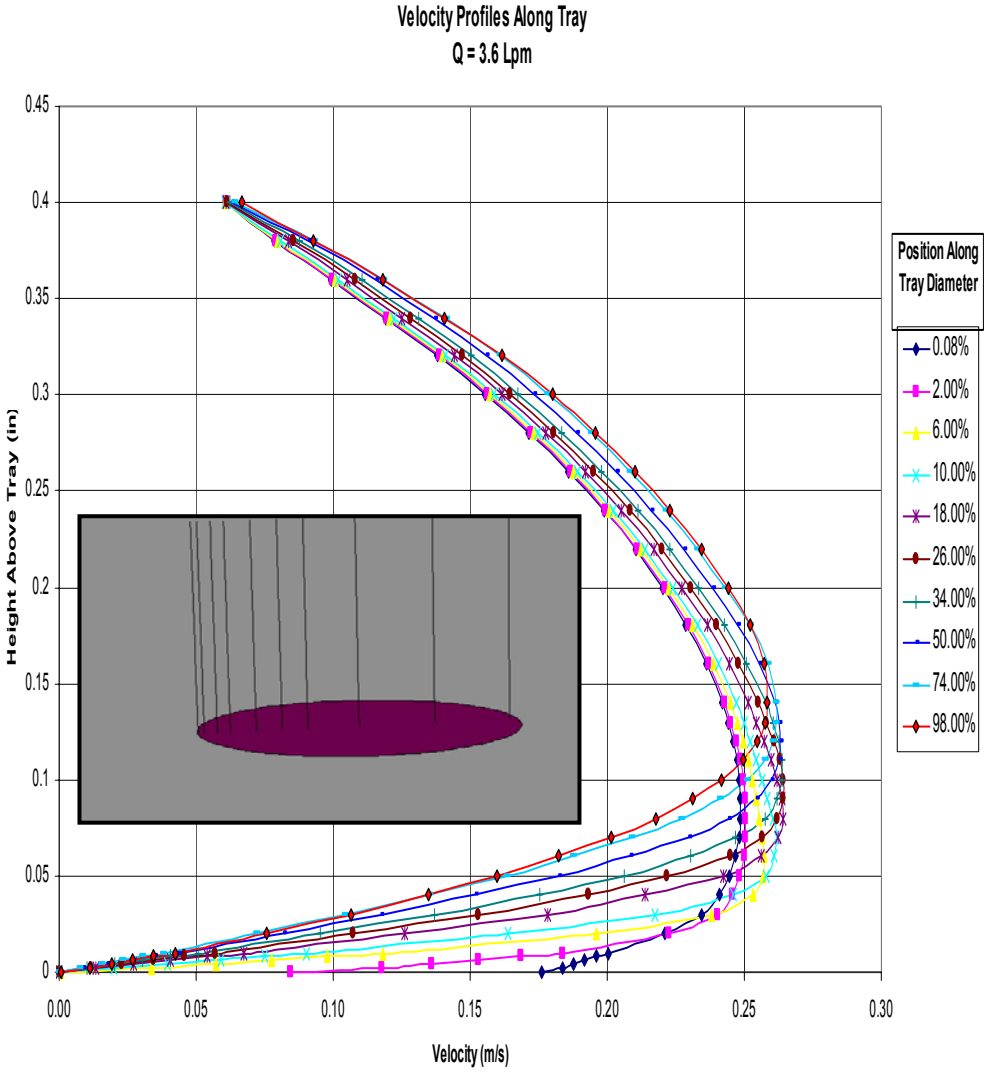

Figure 10. Computational Fluid Dynamics Simulation of Wind Speed at Horizontal Distances along the TGA Sample Pan

- The comparison of measured versus simulated CFD results was very accurate.
- In addition, the measurement of hot wire anemometry wind speeds is very difficult at low velocities and within confined spaces, such as the TGA wind tunnel geometry.
- Therefore, CFD was used to approximate the velocity profiles at other horizontal positions along the plate (sample pan).
- Profiles along the TGA951 Sample Pan for the Q=3.6 LPM case were computed.
- The insert shows the location of velocity profiles relative to the tray, flow is from left to right.

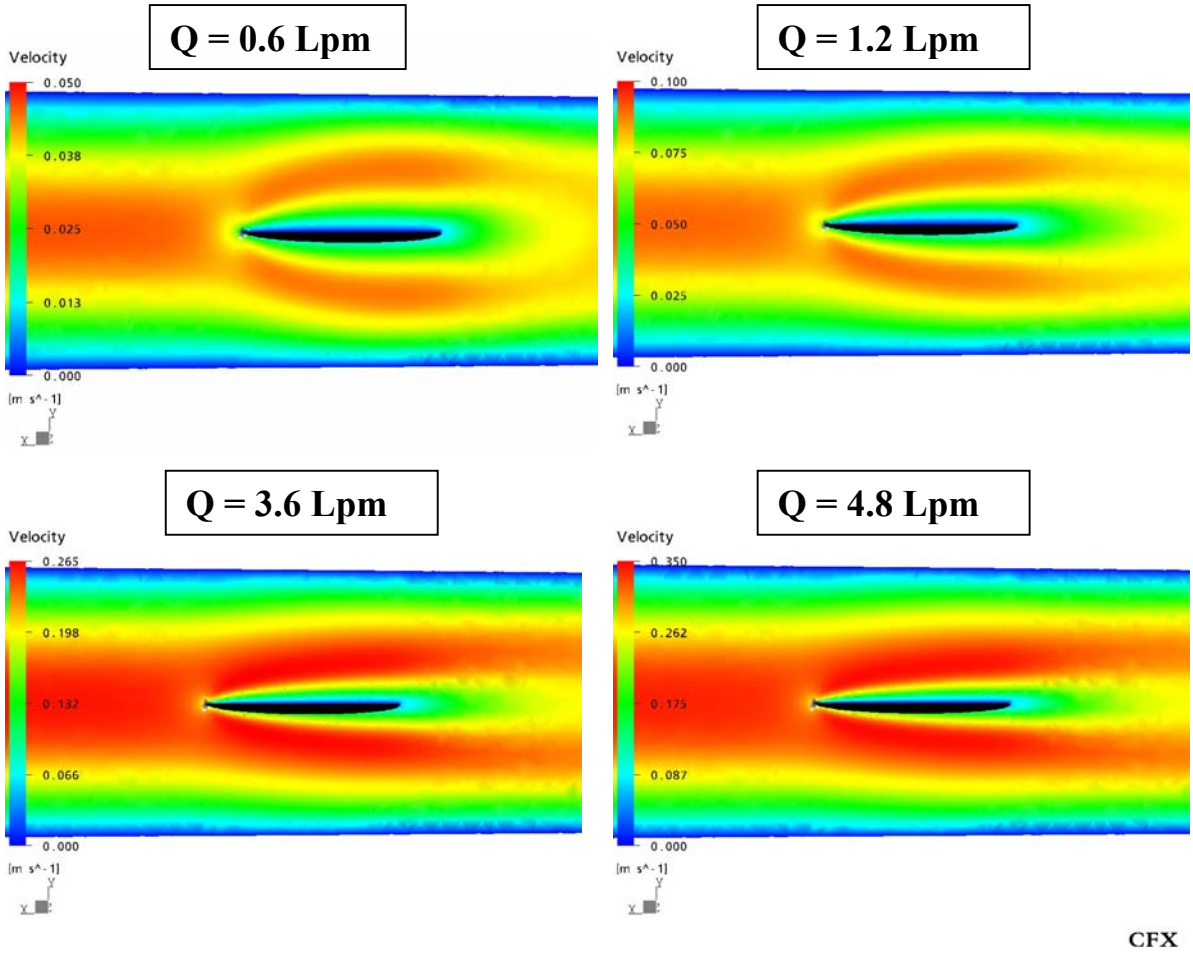

Figure 11. CFD Velocity Contour Plots for the Four Flow Rates: Q = 0.6, 1.2, 3.6 and 4.8 LPM. Note: the velocity scale is different for each flow rate.

- The color-coded velocity values show that the wind speed near the surface of the sample pan is similar to the wind speed near the wall of the wind tunnel tube.

- Therefore, a droplet-material interface on either a suspended sample pan or on the wall (floor) of a wind tunnel will have characteristically low wind speeds associated with a flow velocity approaching a wall.

REVERSE TUBE FLOW WITH SAMPLE PAN: WIND SPEED MEASUREMENTS AND COMPUTATIONS.

Preliminary microbalance experiments have been performed in reverse mode and the next step was to design permanent wind tunnel geometry for the reverse flow, with a coaxial cooling condenser (not shown in any of the figures). The CFD capability was exploited to assist in the design and the 3-dimensional representation of the initial design is shown in Figure 12. The flow patterns for the reverse flow design are shown in Figure 13.

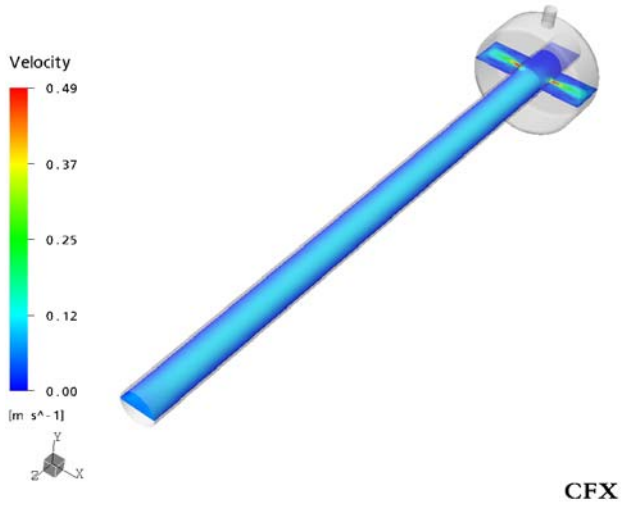

Figure 12. CFD Flow Field and Wind Speed Results in the Horizontal Plane.

The computed estimates demonstrate the expected smooth flow field with a higher velocity near the midpoint. The color-coded velocities are calibrated on the vertical scale. The darker blue flow fields near the outside edge of the tube are at lower velocity than the lighter blue flow field near the center of the tube. The contaminant droplet on a material surface is positioned near the center of the flow in the microbalance tube, therefore, the droplet experiences a velocity that is higher than the mean velocity computed from the flow rate and cross-section.

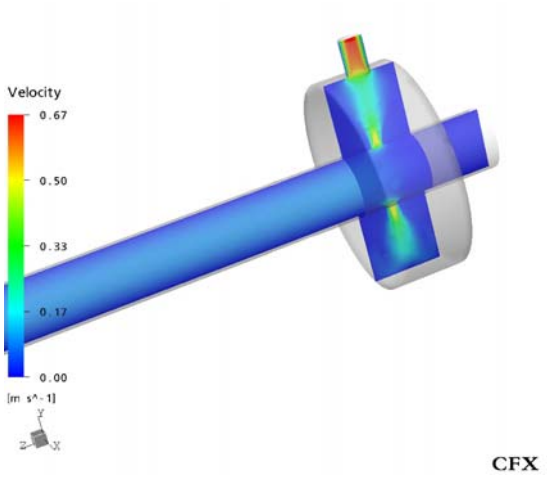

Figure 13. The CFD Vertical Wind Speed Plane Results.

The vertical results are symmetrical with the horizontal flow field, as expected for a tube geometry. Again, a higher wind speed is shown near the centerline where the contaminant droplet resides on the material surface disk. For the orifice sizes in this design, faster flows are shown at the exit from the orifice. The single tube exit to a filter is shown to have an even higher velocity.

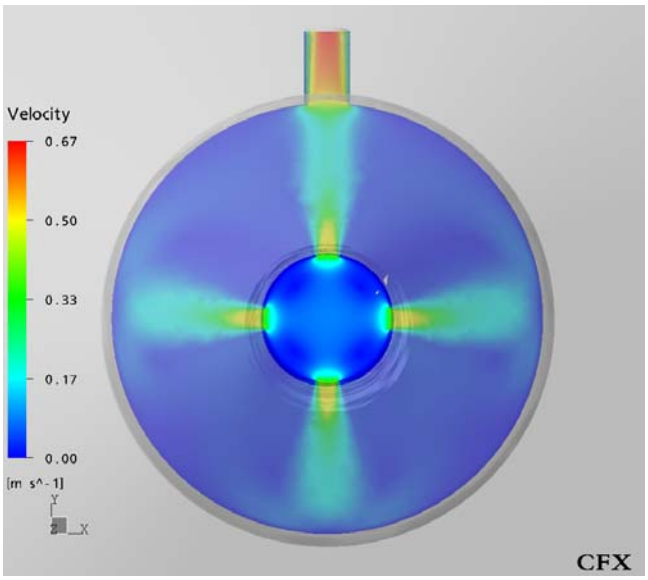

Figure 14. CFD Flow Field Results at the Orifices and Tube Exit.

The wind tunnel flow field is exiting toward the viewer and then turns perpendicular to the wind tunnel flow and out the four orifices. A single tube evacuates the contaminated chemical vapor into a sorbent tube for vapor analysis or a filter system. The CFD velocities show the expected higher rates at the orifice centers and even higher flow rate at the single exit tube.

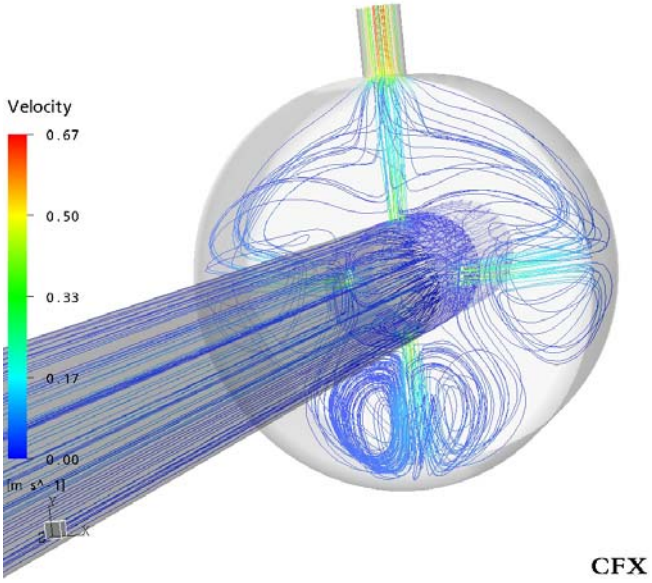

Figure 15. CFD Streamlines in the Wind Tunnel Section and Evacuation Section.

The streamline estimates for the evacuation section are shown to be complex and specific to the orifice position relative to the exit tube. The complex streamlines caused by the exit geometry do not appear to influence the flow field shape or velocity in the measurement section, which is in front of the exit orifice and tube. The measurement section contains the chemical contaminant droplet on a material surface disk.

EVOLVED GAS MICROBALANCE FLOW: MEASURED AND COMPUTED FLOW FIELDS

The Evolved Gas geometry consists of a vertical microbalance design with a horizontal flow field across the droplet and material surface (TA Instruments Model 2950). A diagram of the microbalance and a 3-dimensional CFD representation are shown in Figure 16. The balance mechanism is protected by a low, downward vertical flow. The streamlines for the vertical flow are emphasized in Figure 17. Figure 18 provides a 3-dimensional representation of the flow streamlines and a centered 2-dimensional plane for the wind speed profile calculations. The comparison of the measured versus calculated wind speed profiles is plotted in Figure 19.

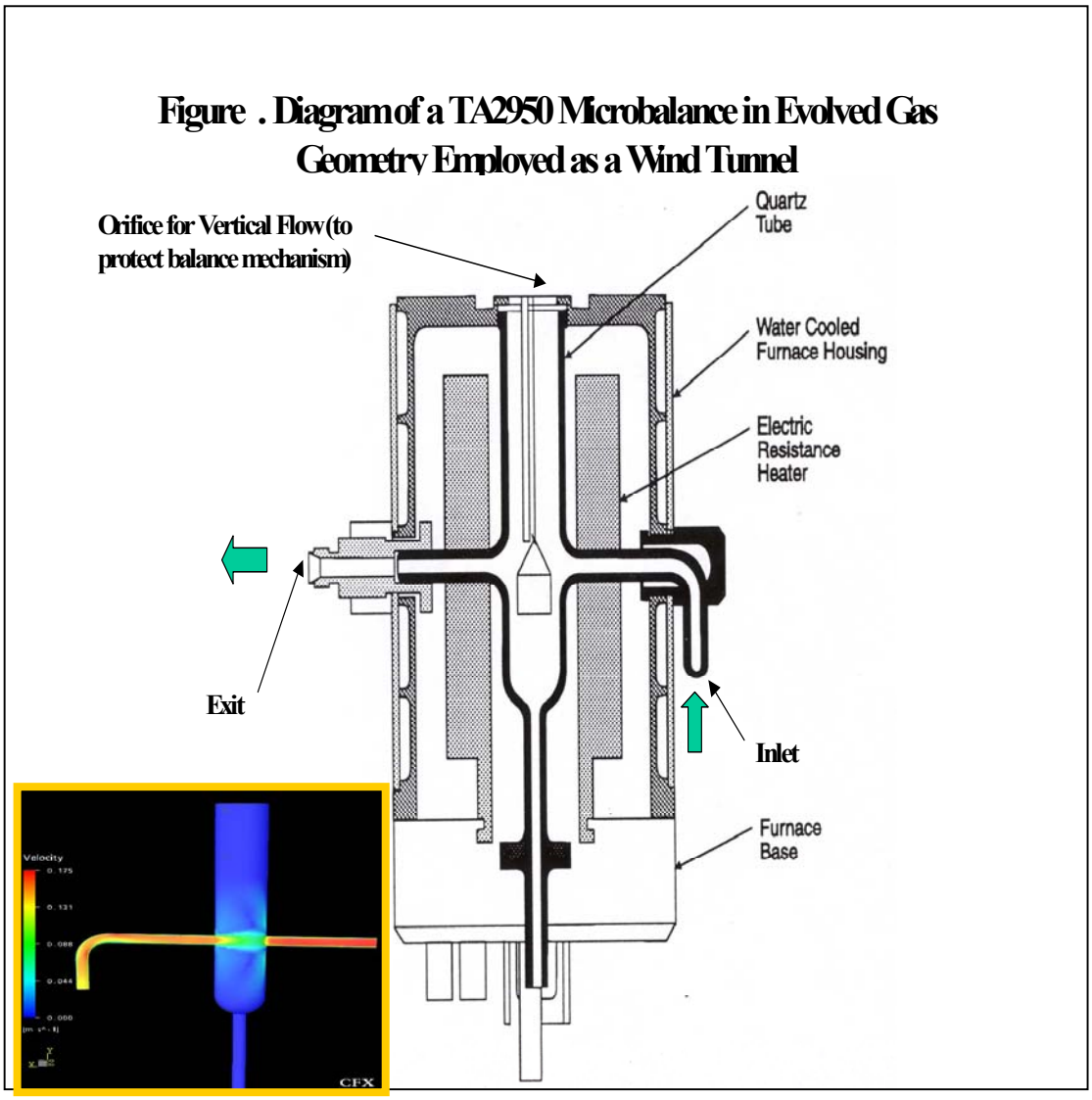

Figure 16. The Diagram of the Evolved Gas Wind Tunnel Geometry of the TA2950 Microbalance is shown in the Larger Figure. The view is rotated by 180 degrees from that in the insert Computational Fluid Dynamics diagram (3-Dimensional Representation.)

- The air enters from the curved tube and flows over the chemical contaminant droplet deposited on the material surface mounted on the balance hang-down wire
- The flow exits through the straight tube.
- The inlet flow passes over the chemical contaminant drop upon a material surface disk (not shown).
- A secondary flow enters from an orifice at the top and flows downward and also exits out the straight tube (on the left in the 2-D diagram, on the right on the 3-D model).
- This downward flow is only for the purpose of protecting the microbalance mechanism from contamination by evaporating or desorbing vapors from the sample pan.
- The ratio of downward to horizontal flow is maintained at a 1/10 flow rate.

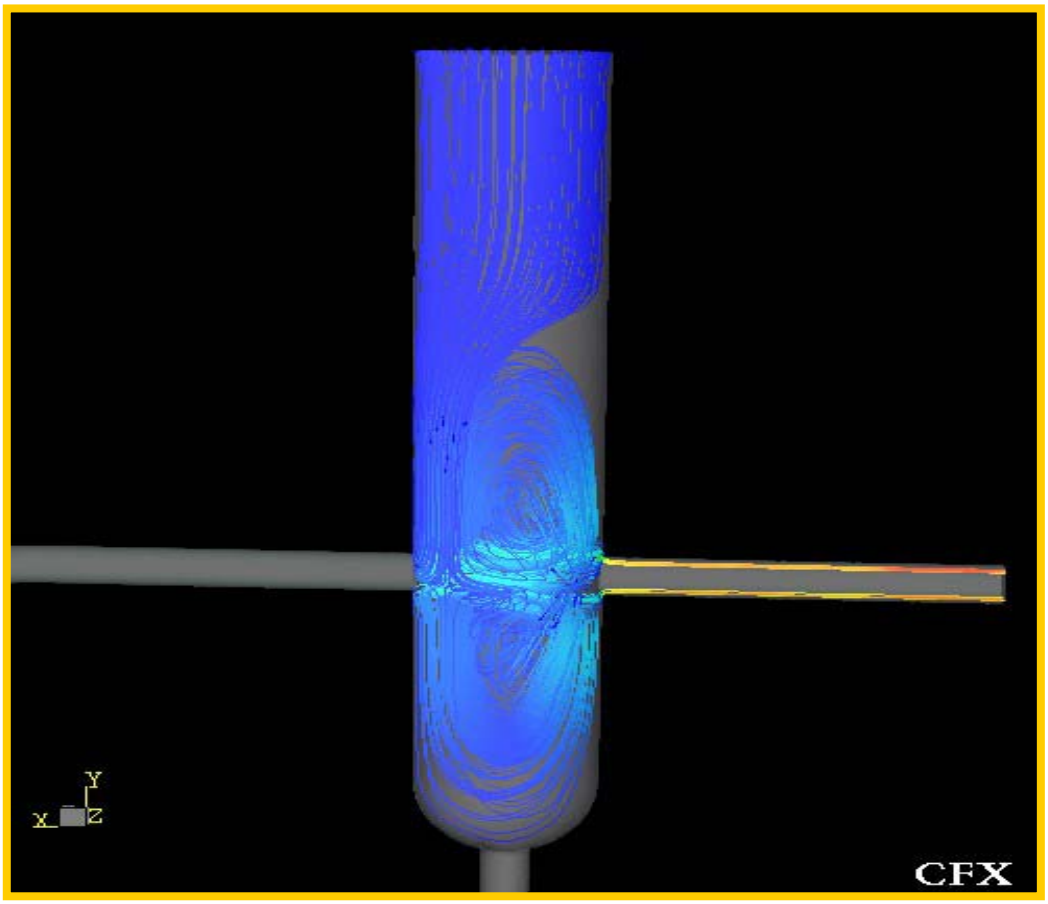

Figure 17. Streamline Close-ups for Various Evolved Gas Microbalance Wind Tunnel Sections

- Computational Fluid Dynamic estimates of streamlines for a variety of 3-D views of the Evolved Gas wind tunnel geometry are shown in the diagram.
- The vertical flow is shown to concentrate toward the wall of the vertical tube.
- A portion of the vertical streamline is shown to bypass the exit tube and flow into the lower chamber of the vertical tube.
- The streamlines then show the flow joins the flow from the upper vertical chamber and enters the exit tube on the right.
- The streamlines show the vertical flow field seems to concentrate near the wall of the horizontal exit tube.
- The horizontal flow from the horizontal inlet on the left expands, as expected, when the flow enters the chamber and contracts rapidly as the flow enters the exit tube.
- The streamlines near the center of the horizontal tube pass over the chemical on the sample disk.
- These streamlines appear to show smooth flow at a wind speed that is lower than the velocity within the closed tube, but higher than the mean velocity based on calculations from flow rate and cross-section of the solid inlet and exit tubes.

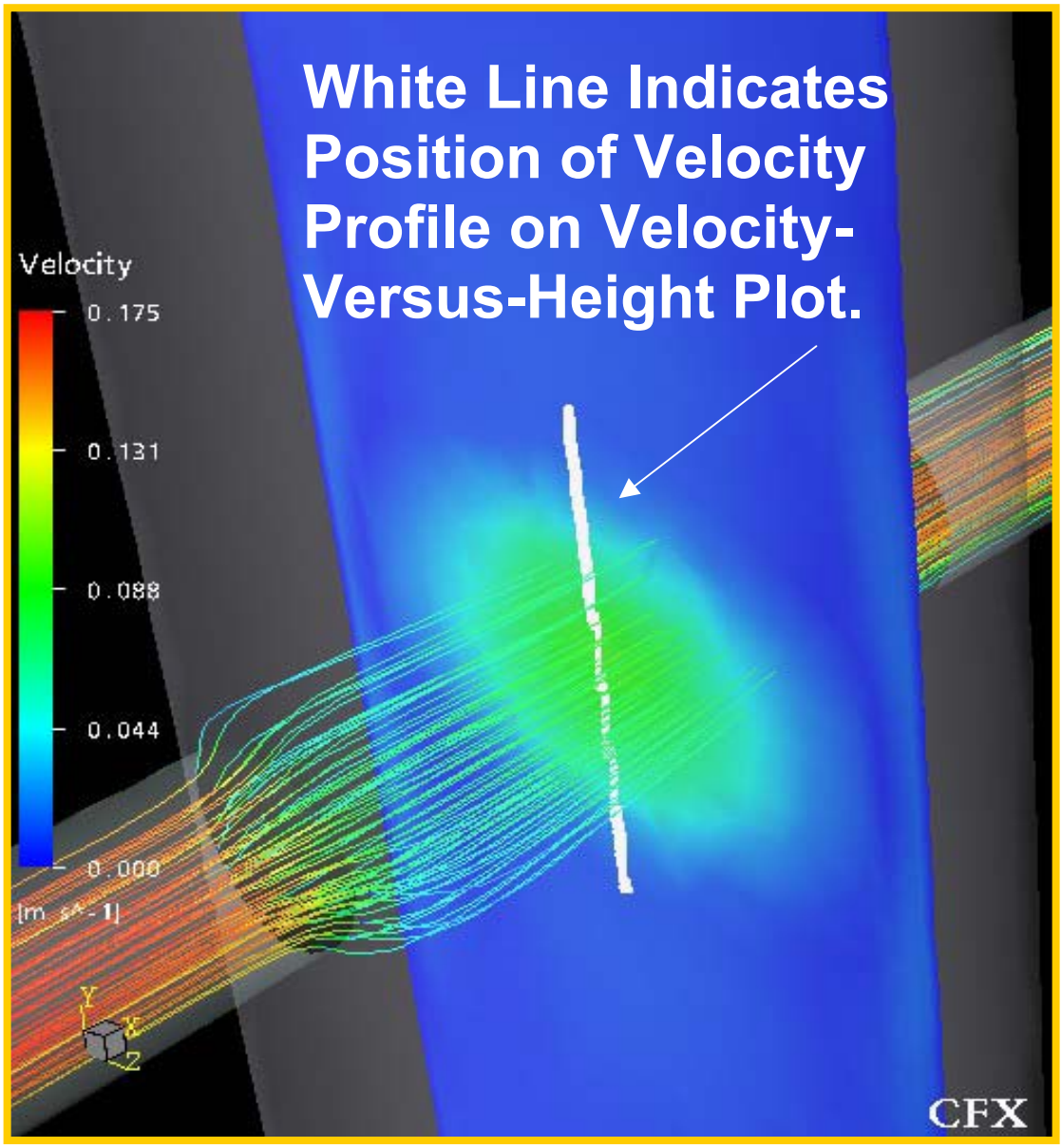

Figure 18. Three-Dimensional Streamlines and Two-Dimensional Plane for the Velocity versus Height Contour Plot

- The 3-dimensional representation of the streamlines show the flow expanding as the flow enters the horizontal microbalance chamber from the inlet tube on the left.
- The color-coded streamlines predict slower wind speeds within the expansion chamber.
- The vertical line shows the plane for the Velocity profile plot.
- The wind speed profile was obtained at the centerline (see “Figure: Wind Speed as a Function of Distance from the Projected Inlet/Outlet Tube Walls of the Evolved Gas Microbalance Wind Tunnel Geometry.”).

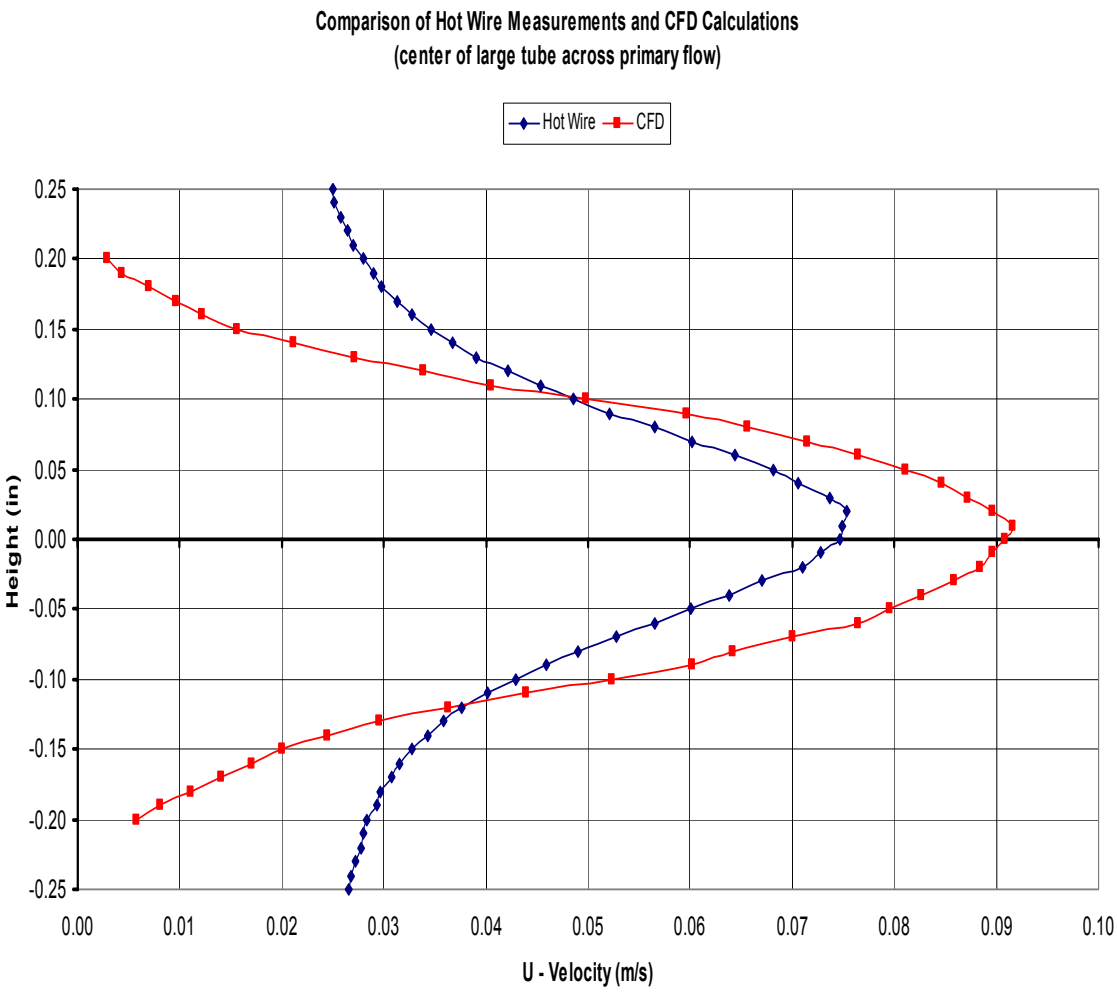

Figure 19. Wind Speed as a Function of Distance from the Projected Inlet/Outlet Tube Walls of the Evolved Gas Microbalance Wind Tunnel Geometry.

- The horizontal, or x-axis, contains the flow velocity in meters per second (m/s).
- The vertical or y-axis contains the distance from the inlet/outlet tube wall in inches.
- This wall diameter is projected into the chamber containing the vertical microbalance sample holder with the droplet on the material surface.
- A characteristic velocity profile results showing the highest velocity at the centerline.
- The centerline velocity is higher than the velocity calculated from the tube cross-section and input flow rate.
- The chemical droplet and material surface disk is at or near the centerline.
- Therefore, the CFD estimates provide an estimate for the actual wind speed at the specimen and guide experimental measurements of the sample wind speed with a hot wire anemometer.

SUMMARY

Based on an evaluation of pesticide transport testing, the flow field of interest in a laboratory wind tunnel for evaporation and desorption from the liquid to the vapor state is the molecular level boundary layer at the liquid-vapor interface rather than a macroscopic vapor-vapor diffusion processes.

Microbalance instruments configured in a wind tunnel geometry have been demonstrated to allow measurements of droplet weight-loss vs time of good reproducibility and low 95% confidence interval for sessile droplets on polyurethane coatings (CARC). These measurements on neat and thickened HD and GD allow one to distinguish between liquids with similar vapor pressures and rank various chemicals in terms of persistence and vapor hazard. Mean wind speeds of 0.17 and 0.04 mph were employed.

Low level wind speed measurements needed for environmental fate wind tunnel experiments can be extended down to 0.05 m/s (0.11 mph, 0.186 Kph), by employing a special low-pressure calibration method and a small hot wire anemometer.

Wind speed profiles have been measured for microbalance tube sample pan and vapor sampling wind tunnels employing a miniature hot wire anemometer mounted onto a micro-positioning instrument.

Characterization of the wind speed at the interface between the contaminant droplet and the surface material is critical to environmental fate experiments. Measurements of distances of only 2.54 mm (0.1 inch) from the wall or sample pan were completed without damage to the hot wire anemometer. Errors due to heat flow from the hot wire anemometer to the wall were detected and corrections were applied.

Wind tunnel geometries relevant to environmental fate droplet-surface interactions were successfully coded into Computational Fluid Dynamics software to predict 3-dimensional flow velocities and streamlines. General agreement was obtained between the micro-positioned anemometer measurements and predicted values. Therefore, the Computational Fluid Dynamics simulations are being applied with increased confidence to characterize the full microbalance flow field for the tube geometry with center sample pan and the evolved gas geometry.

ACKNOWLEDGEMENTS

The authors appreciate useful discussions with Dr. Russ Seebaugh, Science and Engineering Associates, Inc. and Dr. R. Nickol, GEO-Centers Inc. The authors would also like to acknowledge program support and assistance from Dr. H. Dupont Durst and Dr. Frank Verderame, ECBC

REFERENCES

1. Shuely, Wendel J., McHugh, Vincent M., and Ince, Brian S., "Investigation of Diffusion and Evaporation of Liquids from Polymeric Substrates Under Environmental Conditions Employing Computer-Controlled Thermogravimetric Instrumentation", American Chemical Society Abstracts of Papers, COMP 84, August 1984.
2. Shuely, Wendel J., and Ince B. S., "Thermogravimetric Method for Measurements of

Equilibrium and Transport Properties Relevant to Chemical-Polymer Compatibility Evaluation" in the Proceedings of the 22nd Conference of NATAS, p 354-259, September 1993.
3. Shuely, Wendel J., "Standard Test Methodology for Measurement of Polymer Solubility, Equilibrium Sorption and Desorption Diffusion Coefficients for Hazardous Liquids," Proceedings of the Symposium on Performance of Protective Clothing: Improvement Through Innovations," J. Johnson and Z. Mansdorf, Ed., American Society for Testing and Materials, January 1994, Philadelphia, 19103.
4. Thibodeaux, Louis J. Environmental Chemodynamics. Movements of Chemicals in Air, Water, and Soil. Wiley Interscience Publication. New York. 1996.
5. "Wind Tunnel Model Studies of Buildings and Structures", ASCE Manuals and Reports on Engineering Review Practice No. 67, 1987.
6. Cermak, Jack E., "Wind Tunnel Design for Physical Modeling of Atmospheric Boundary Layer," *Journal of the Engineering Mechanics Division*, ASCE, Vol. 107, No. EM3, Paper 16340, June 1981, pp. 623-642.
7. Cermak, Jack E., "Laboratory Simulation of the Atmospheric Boundary Layer", *AIAA Journal*, AIAA, Vol. 9, No. 9, September, 1971, pp. 1746-1754.
8. Shevell, Richard S., Fundamentals of Flight, Prentice-Hall, Inc, Englewood Cliffs, NJ, 1983, pp. 162-163.
9. Barlow, Jewel B.; Rae, William H., Jr; and Pope, Alan; Low-Speed Wind Tunnel Testing, 3rd Edition, John Wiley & Sons, Inc., NY, 1999, pp. 654-655.